Towards the adaptability of coastal resilience: vulnerability analysis of underground gas pipeline system after hurricanes using LiDAR data

Xiameng Huang

Assistant Professor, School of Navigation Engineering
Guangzhou Maritime University
101 Hongshansan Road, Huangpu District,
Guangzhou, Guangdong, 5000012, China
Email: xiamengh123@163.com

Jie Gong

Associate Professor, Department of Civil & Environmental Engineering
Rutgers University-New Brunswick
Piscataway, New Jersey, 08854, United States,
Email：jg931@soe.rutgers.edu

Peifeng Chen

Associate Professor, School of Public Policy and Administration
Chongqing University
174 Shazheng St,
Chongqing, 440044, China
Email: iseesee@126.com

Xuan Hu*

Assistant Professor, School of Public Policy and Administration
Chongqing University
174 Shazheng St,
Chongqing, 440044, China
Corresponding Email: hugoshawn@gmail.com

Acknowledgments

This study is supported by the National Natural Science Foundation of China (71904020), and Chongqing University (2019GGXY00).

Abstract

The coastal pipeline is subjected to threats after extreme coastal weather events, however, most of the extant work fails to include pipeline risk assessment in the post-disaster coastal resilience evaluation, because the labor-intensive and time-consuming pipeline risk analysis techniques cannot be readily extended for disaster application. To address this need, this study exploited Light Detection and Ranging (LiDAR) data for the vulnerability analysis of underground gas pipeline system after hurricanes. Specifically, compared to the prevailing work that is emphasized on the accuracy, this studied identified three requirements for disaster response applications including rapidity, applicability, and operability. Upon these requirements, we integrated LiDAR data with geospatial processing tools in ArcGIS to identify the most vulnerable location in the pipeline system aftermath of hurricanes in coastal community. The method is implemented to cope with four facets of threats (vertical displacement, lateral deformation, flooding, and aging effect) and validated using a hurricane Sandy case study in Ocean County, New Jersey. The results showed that the proposed method not only satisfies the above three requirements in disaster response, but also aligns with the observed hurricane-induced damage patterns, and therefore deem appropriate for vulnerability analysis of underground gas pipeline system after hurricanes.

Keywords: coastal resilience, gas pipeline, vulnerability, hurricane, risk assessment

1. Introduction

Volumes of scientific evidence and data suggest extreme coastal weather events will continue to multiply and intensify (Hassanzadeh et al., 2020; Ting et al., 2019; Wang and Toumi, 2021), increasing coastal resilience to these threats is a global concern (Barbier, 2014). Compared to extensive studies on the resilience of communities (Huang et al., 2021) and building infrastructures (Zhou et al., 2019), the resilience of underground pipeline systems is understudied. Although considered as the safest means for transporting energy fuels (Zakikhani et al., 2020), in facing extreme events such as hurricanes, the damage, and failure of the transmission pipeline networks can lead to life-threatening secondary hazards (e.g. gas leak, gas explosion). For instance, the 1994 flooding in Houston, Texas exposed 17 underground pipelines, four of which broke (NTSB, 1996). Ignition from gasoline has caused 547 people to receive burn and inhalation injuries causing an estimation of $16 million losses. Moreover, increasing demand for energy consumption is resulting in more extensions on the pipeline network systems as well as more people living and working closer to pipelines. Given that hurricanes induced wind, flooding, and storm surge, as well as internal corrosion could pose an undue threat to human lives and properties, understanding the resilience of underground gas transmission system aftermath of an extreme coastal event is of remarkable interest to improve the coastal resilience.

The extant studies on investigating the failure mechanism of the pipeline system can mainly be categorized into five types including mechanical, operational, corrosion, natural causes, and third party activity (Davis et al., 2006). Regardless of the type, these studies address the capability perspective of coastal resilience by identifying the potential risk caused by the defect in design, malfunctions in operation, and time-dependent deterioration through careful inspection, monitoring, testing, and analysis. Upon such formulation, pipeline risk analysis requires an extensive in-line inspection and monitoring of pipeline conditions to ensure accuracy and to minimize the uncertainties of the results (Zakikhani et al., 2020). For instance, extensive studies are built based on high precision measuring tools (Lee et al., 2013; Shi et al., 2015), comprehensive signal processing techniques (Chen et al., 2010; Saha et al., 2010), and sophisticated failure analysis models (Farrag and Gong, 2016a; Jin et al., 2014; Lee et al., 2013). Combined, these works provide a holistic view of underground pipeline system resilience from the capability's perspective, however, few of them emphasize the other dimension of coastal resilience, adaptability.

Differently, adaptability emphasizes the ability of a system to respond and adapt to changes caused by natural disasters or incidents. Rather than accuracy, which is often time-consuming, adaptability requires identifying the vulnerability of the pipeline system in an efficient way to develop coping strategies. In such a sense, despite all efforts from the literature on capability-centric pipeline risk assessment methods (Lee et al., 2013; Shi et al., 2015), they cannot be extended to address the adaptability for disaster response applications. In all, the adaptability-centric analysis should address three issues: rapidity (Linnenluecke and McKnight, 2017), applicability (Elaine Daily and Padjen, 2010), and operability (Huang and Lien, 2012). Particularly, disaster is characterized by a highly time-sensitive environment (Hu and Gong, 2019a). To make sufficient time to inform residents to respond, the rapidity rather than the accuracy should be stressed. Moreover, the applicability requires that the methods need to build upon the availability and feasibility of risk detection techniques. Put differently, tools such as ultrasonic, magnetic flux are considered expensive, time-consuming, and unsafe to operate (Xie and Tian, 2018), and therefore may not be applicable for pipeline risk assessment for the disaster response purpose. Last, different from the laboratory experiments environment, the practicability demands that the productivity of the method should be prioritized – this is to say a well-develop platform might be considered as a baseline for the analysis.

Underneath the specific requirements that disaster response has to address, we find that integrating geographic information systems (GIS) with remote sensing data may offer a solution. Regarding operability, GIS is widely employed as decision support tools because the technology can support the fusion of data from multiple sources and meanwhile has the capability of spatial analysis, visualization, which is considered critical for disaster response (Gunes and Kovel, 2000). Moreover, compared to an onsite survey or in-line inspection, spatial data are more widely available (Zerger and Smith, 2003) as collecting remote sensing data has become a routine survey after major disasters (Huang et al., 2021). For instance, in addressing Hurricane Sandy alone, within the three days of the disaster stroke, there are at least three Light Detection and Ranging (LiDAR) datasets available, including pre and post-Sandy LiDAR data from USGS EAARL-B (Experimental Advanced Airborne Research Lidar) Lidar system, post-Sandy LiDAR data from USACE (United States Army Corps of Engineers) NCMP (National Coastal Mapping Program). Regarding the practical perspective, the GIS system has proved successful and productivity in numerous disaster scenarios such as flood risk mapping (Liu et al., 2003; Tran et al., 2009), resource allocation (Chen et al., 2011; Fiedrich et al., 2000), evacuation planning (Font et al., 2010; Kucera et al., 2004; Zou et al., 2006), landslide susceptibility mapping (Cevik and Topal, 2003), etc. Drawing upon the rapidity, operability, and practicality for pipeline risk assessment during disasters, the paper deals with an overarching research question:

What is the pipeline risk assessment method to address the rapidity, operability, and practicality requirements in disaster response?

To address the research question, this study investigates the integrating of spatial data and GIS for the pipeline risk assessment in disaster response. Building upon the five pipeline failure mechanism, the assessment method exploits the remote sensing LiDAR data and inventory data to identify four facets of damage patterns including vertical displacement caused by erosion and soil movement, wind and surge induced horizontal displacement, flooding, and aging effect. Then, the proposed method is implemented in GIS and empirically validated using Hurricane Sandy data.

The remainder of this article is structured as follows. Related literature is presented in Section Two, followed by the introduction methodology of this study in Section Three. The proposed method is validated through empirical data from Hurricane Sandy in Ocean County, New Jersey, which is presented in Section Four. The results and discussion is presented in Section Five and the study is concluded thereafter with implications in the final section.

2. Literature review

2.1 Defect detection based method

Defect detection is a process of exploiting different types of tools to identify the damage cues, which provide the first diagnosis of the gas pipeline system. Traditionally, the objective of this process is to maximize the detection accuracy with minimum uncertainty (Zakikhani et al., 2020), which is relied on the accuracy of the pipeline damage data obtained through inspection, monitoring, testing, and analysis techniques. In doing so, numerous studies are exploring the state of art high-precision tools for pipeline leakage detection such as magnetic flux (Gloria et al., 2009), ultrasonic (Alobaidi et al., 2015), Electromagnetic acoustic transducers (EMAT) (Hirao and Ogi, 1999), etc. Nevertheless, these In-line inspection technologies are proved accurate in defect profiling, there are limitations for extending them for disaster response applications. First, the rapidity issue of employing these high-precision tools in pipeline risk analysis in disaster response is unaddressed in literature. Specifically, disasters are characterized with time-sensitive environment (Hu and Gong, 2019b) and there is only a narrow time window for response actions (Standard, 2001), which in turn call for rapidly identifying the potential risk that could lead to life-threatening secondary hazards (e.g. gas leak, gas explosion). On the other hand, high-precision damage detection tools often require complex data collection procedures (e.g., frequent on-site inspection, data validation), which is often accompanied by extensive time and intensive labor (Zakikhani et al., 2020). To this end, these high-precision tools might address the rapidity for pipeline risk assessment during disaster response at the first place. Second, the applicability of these tools is under questioning because these tools are designed to focus on specific types of pipeline defect. For instance, magnetic flux are typically applied to detect metal loss (e.g. corrosion). A review of current MFL applications in detecting corrosion is elaborated in Vanaei et al. (2017). Crack, on the other hand, is best detected using ultrasonic (Lee et al., 2010). and EMAT(Dixon et al., 2011). Regarding the disaster-induced geometry changes, Xie and Tian (2018) argued that the feasibility of these technologies is unravelled because in some studies these tools are reported to be capable of detecting this type of flaw while in other studies not. In such a sense, alternative sensors for the geometry changes measurement require further investigation. Last but not least, the operability demand in place algorithms and well-developed platforms. Nevertheless, the analysis requires sophisticated signal processing algorithms, such as wavelet transform (Saha et al., 2010), split-spectrum processing(Saniie et al., 2012), artificial neural networks (ANNs) (Carvalho et al., 2006). Despite their success in the experiment stage, the validation in practise is understudied. All combined, the rapidity, applicability and operability implies that high precision tools are not the candidate to address the pipeline risk assessment aftermath a disaster.

2.2 Risk analysis based method

Alternatively, other scholars integrate historical data and expert experience into the risk analysis to improve the understanding of the resilience of the underground pipeline system. Risk analysis aims to estimate the probability of failure and assess its consequences (Aljaroudi et al., 2015). Depending on the source of input data, risk analysis can be divided into quantitative methods and qualitative methods (Han and Weng, 2011). While quantitative methods are mainly built upon objective data, qualitative methods incorporate judgment from the experts to the analysis. The quantitative method assesses risk by numerical simulation, including a quantitative calculation of possibilities and consequences of different accidents (Han and Weng, 2011). Mathematic modeling is a quantitative method that relies largely on objective data. For instance, Aljaroudi et al. (2015) and Jo and Ahn (2005) proposed quantitative risk analysis models that integrating historical data with disaster data. However, both models are too complicated to operate because more than 50 pipeline parameters are required as inputs and their sources are not elaborated. Xie and Tian (2018) further underscored that the completion of the pipeline data is a major concern because it requires a considerable amount of inputs even the pipeline operators do not have. On the other hand, historical data are widely available, and therefore are fitted in prediction models such as the markovian prediction model (Sinha and McKim, 2007), support vector machines (SVM) (Lee et al., 2013), Genetic Algorithm (GA) based models (Tee et al., 2014) (208), finite element model (FEM) (Jin et al., 2014). Nevertheless, given that coastal extreme events are more uncertain than predictable (Lin et al., 2012), the historical data-centric model is deemed ineffective in reflecting the real disaster situation. Admittedly, these models provide very detailed results if the input data is sufficient, the feasibility of collecting a timely data environment remains unravelled in literature. Alternatively, expert judgments are implemented into risk-based assessment for qualitative measurement. To obtain the qualitative risk value, numerous approaches were proposed including Analytic Hierarchy Process (AHP) (Cagno et al., 2000), Fuzzy logic method (FL) (Jamshidi et al., 2013), Fault Tree Model (FTM) (Yuhua and Datao, 2005), etc. While these approaches are good at identifying the causes, Han and Weng (2011) argued that they fall short in assessing the risk.

2.3 Remote sensing based method

Remote sensing data are increasingly deployed for coastal resilience applications because the technique is capable of acquiring real-time or near-real-time disaster data for situational awareness (Hu and Gong, 2018). Compared to the high-precision defect detection tool, remote sensing sensors that are often mounted on aircraft are capable of covering thousands of miles. Therefore, it is deemed a solution for pipeline risk assessment in disaster response(Roper and Dutta, 2005). Among all the remote sensing techniques, light detection and ranging (LiDAR) is broadly studied for pipeline risk assessment because of its high accuracy (Hodgson and Bresnahan, 2004) and visibility (Kumar et al., 2017). In addition to visual inspection (Piciarelli et al., 2018), LiDAR is a method for determining ranges, which has already been applied for quantifying the different types of morphologies in the coastal community such as dunes(Rango et al., 2000), vegetation(Campbell et al., 2018), building infrastructure (Hatzikyriakou et al., 2015), and water bodies (Canaz et al., 2015). Furthermore, by comparing two datasets (e.g., pre-disaster and post-disaster), called change detection, the technique is able to identify the volumetric changes in the morphology. For instance, Roper and Dutta (2006) proposed using change detection of before and after aerial imagery data for pipeline damage assessment caused by ground deformation. Similar change detection investigations are carried out using LiDAR data such as Tao and Hu (2002), Zhou et al. (2016a). Besides, other scholars attempt to compare the pipeline damage correlations obtained from both image data and LiDAR data (Toprak et al., 2018). In sum, remote sensing techniques have proved the success of providing a reliable recording of the coastal morphologies and measurements of changes, it is worthwhile mentioning that most of these metrics are built upon Vertical Displacement, investigation on other geometric changes remains scant. Nevertheless, pipeline systems are also subjected to horizontal loads (e.g., wind load, soil load) (Wang et al., 2020; Zeng et al., 2019), flooding loads (Li et al., 2017), and the aging effect (Dahire et al., 2018), which requires further investigations.

3. Methodology

The methodology is articulated into two steps (as depicted in Figure 1) including threats measurement and vulnerability analysis. The method is implemented through a Python procedure in ArcGIS.

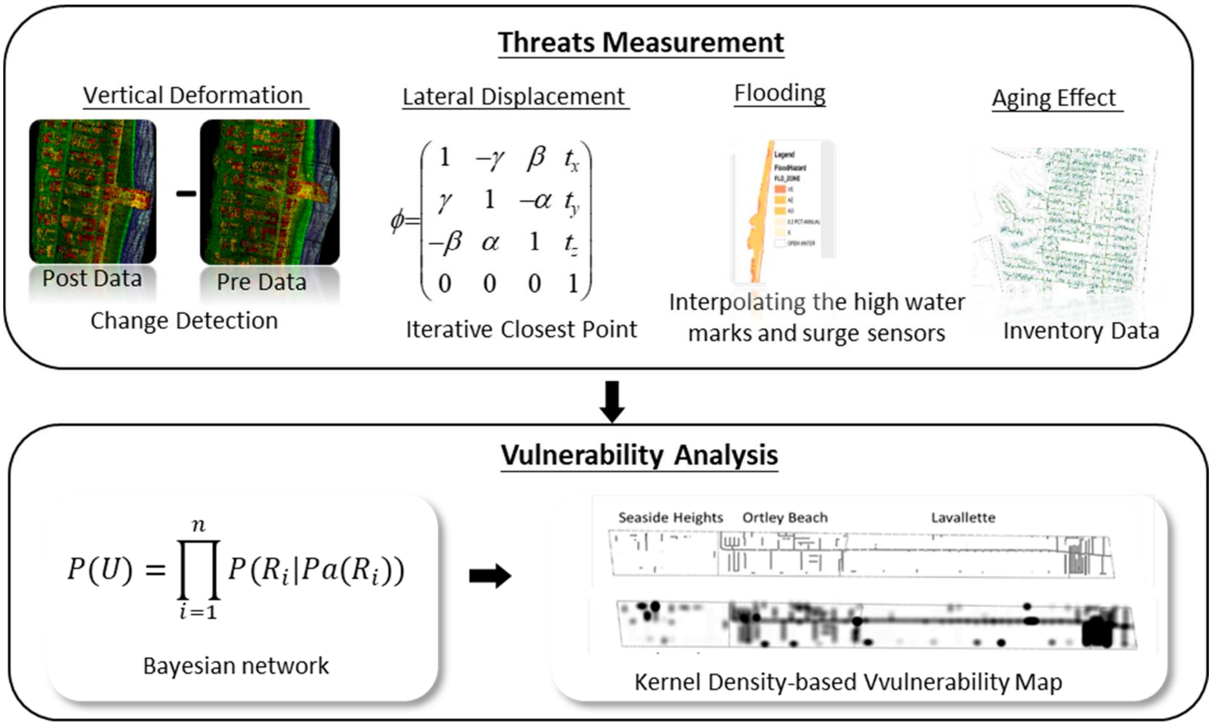

Figure 1 The methodology

3.1 Threats measurement

As mentioned earlier, high precision pipeline defect detection tools such as magnetic flux (Gloria et al., 2009), ultrasonic (Alobaidi et al., 2015) are proved high accuracy, however, they fail to address the rapidity, operability, and practicality issues associated with disasters. Alternatively, remote sensing data are deployed for real-time or near-real-time pipeline threats measurement. In sum, four types of threats are considered in this study to identify the most vulnerable location in the pipeline network (Table 1). These four threats are determined by both the capability of LiDAR data and the damage mechanism of hurricane disaster. On the one hand, a hurricane is considered as a combined wind and surge event (Lin et al., 2012), which will further introduce wind-induced vibration (Wang et al., 2020) and flooding load (Li et al., 2017) to the coastal zones. At the same time, the vertical soil movement (Zeng et al., 2019) such as the landslide and the aging effect (Dahire et al., 2018), of the pipeline system could also impose a risk on the resilience of the pipeline system. On the other hand, LiDAR data is deemed effective and efficient in morphology mapping, which is capable of capturing the disaster-induced geometry changes on the coastal zones (Tatui et al., 2019). By correlating the pipeline damage with the ground deformation, the disaster-induced pipeline risk can be identified (Roper and Dutta, 2006). The detailed methods to measuring the four threats are elaborated in the following sections.

Table 1 Threats from Extreme coastal weather events

Threat	Source of damage	Asset Type	Influencing Factors	Disaster Evidence
Vertical Displacement	Soil settlement, landslides	Underground mains & services; Aboveground gas meter sets & regulators.	Area topography and soil type, Pipe vicinity to hazard & orientation; Pipe type, size, and Age, Joint type.	Change Detection of Pre- and post-airborne LiDAR data
Lateral displacement	Wind-induced vibration or earth movement	Majorly aboveground gas meter sets; Underground pipeline	Tornado & hurricane risk areas; Facility's vicinity to hazards; Aboveground facility structure type	Integrating Iterative Closest Point (ICP) with kernel interpolation using Pre- and Post-Airborne LiDAR data
Flooding	Hydrostatic (buoyancy or flotation effect) , breaking wave	Underground mains & services; Aboveground gas meter sets & regulators.	Area topography and soil type; Pipe vicinity to hazards and soil; Cover; Gas meter height above ground; Cast iron Joint type and pressure	Flood inundation map (e.g., Interpolation from watermark, Satellite-Based Flood imagery)
Aging	Aging induced cracking and deterioration	Majorly underground pipeline; Aboveground gas meter sets	Pipe type, size, and Age, Joint type; Construction year.	Inventory Data

3.1.1 Vertical Displacement

The vertical soil movement, such as settlement or landslides, is commonly occurring during natural disasters. These vertical movements may result in sudden pipe collapse, gas leak, or significant deformations that induce long-term stresses on the pipe. Secondary effects of the earth movement include scour, erosion, and reduced soil cover, which may lead to risk increasing in excavation damage and pipe exposure. An increase in the overburden stresses on the belowground pipes may also result from the accumulation of soil and debris above the pipe.

The Vertical Displacement of the soil is measured using change detection by the comparison of the pre and post-airborne LiDAR data. A detailed description of the procedure for our change detection is described in Zhou et al. (2016b). Both pre and post LiDAR datasets are classified as ground and non-ground objects using a progressive morphological filter algorithm (Zhang et al., 2003). Then, a point-to-point-based algorithm is adopted to calculate the distance between two data sets. The distance between two datasets $\{\boldsymbol{P},\boldsymbol{Q}\}$ at location i is expressed by the following equation:

$$D_{vert,i} = \min_{i'} \| p_i - q_{i'} \|$$

Where $p_i \in \boldsymbol{P}$, $q_{i'} \in \boldsymbol{Q}$, i and i' are the corresponding location in the pre-disaster dataset $\boldsymbol{P}$ and post-disaster dataset $\boldsymbol{Q}$, respectively.

$D_{vert,i}$ is the vertical displacement between pre and post datasets at location i.

3.1.2 Lateral Deformation

The lateral load, such as wind load or debris flow, exert three types of forces on the building envelop including uplift load, shear load, and lateral load. The deformation of the building will further cause collaborative damage to the pipeline system attached to them. Though there are numerous studies addressing the measuring of the earthquake-induced lateral deformation (Glisic and Yao, 2012; Toprak and Taskin, 2007), these studies cannot be extended for the hurricane-induced horizontal movement on the pipeline because the damage mechanism is significantly different. One exception is the work by Zhou et al. (2016b), who used change detection to identify the hurricane-induced horizontal deformation. However, the authors' assumption is that the pipeline facilities are considered to be rigidly attached to the building envelope, which only holds for the aboveground pipeline.

Compared to the Vertical Displacement, the lateral movement of the soil is more strenuous to obtain. This study adopted an Iterative Closest Point (ICP) algorithm proposed by Nissen et al. (2012). The lateral deformation is computed as the squared sum of the distances between each source point p_i ($p_i \in \boldsymbol{P}$) and its corresponding targeted point $q_{i'}$ ($q_{i'} \in \boldsymbol{Q}$). The distance lateral deformation is measured using the equation below:

$$D_{lat,i} = \min(\sum_i \|(\phi p_i - q_{i'})n_i\|^2)$$

Where $p_i \in \boldsymbol{P}$, $q_{i'} \in \boldsymbol{Q}$, i and i' are the corresponding location in the pre-disaster dataset $\boldsymbol{P}$ and post-disaster dataset $\boldsymbol{Q}$, respectively.

$D_{lat,i}$ is the lateral deformation between pre and post datasets at location i.

n_i denotes the normal to the tangent plane at $q_{i'}$;

ϕ denotes the rigid body transformation, here,

$$\phi = \begin{pmatrix} 1 & -\gamma & \beta & t_x \\ \gamma & 1 & -\alpha & t_y \\ -\beta & \alpha & 1 & t_z \\ 0 & 0 & 0 & 1 \end{pmatrix}$$

t_x, t_y, t_z are the translation in the x, y, z direction and α, β, γ are the rotation about the x, y, z axes respectively.

3.1.3 Flooding

Flood water can create loadings (e.g., hydrostatic, breaking wave, hydrodynamic, debris impact) on the underground pipeline. The flooding loads dependent on the flood depth. The rise of the water table in flooding zones can result in a net upward force on the buried pipe when the buoyancy force exceeds the downward weights of the pipe and soil column above the pipe. In particular, in low-pressure cast iron's mains pipeline, water may intrude inside the pipe through the joins if the water head above the line is higher than the internal pressure of the pipe. Water levels that cover gas service meters and regulators may also present safety risks. Besides, heavy rains may expose underground pipelines in areas susceptible to soil erosion; thus subjecting the lines to other threats such as corrosion and excavation damage.

Flooding height data are created from filed verified high watermarks and storm surge sensors. In this study, the flooding height data is obtained from the FEMA Modelling Task Force (MOTF) map, in which a flooding map is produced by interpolating the high water marks and surge sensors and then subtracting them to the Digital Elevation Model (DEM).

3.1.4 Aging effect

Another threat to the pipeline network comes from the long-term aging effect. Aging infrastructure is a common phenomenon in the U.S. Among them; it is reported that more than half of the U.S. gas pipelines are over 45 years old. Danger lurks underground from these aging gas pipeline systems. The long-term changes such as the construction of aboveground structures creep process in the soil as well as long-term fluctuation of the temperature, could cause a pipeline bending strain. Once this strain is coincident with other pipeline defects, the tensile strain may speed up the deterioration of the pipeline. In this study, the age of the pipeline is obtained based on the inventory data.

3.2 Vulnerability analysis

In this study, service pipelines and main pipelines are evaluated differently in the risk analysis. For the service pipelines that connect distribution pipelines to a meter and deliver natural gas to houses, only the risk of their defect is considered. However, for main pipelines that connect high-pressure transmission lines and low-pressure service lines, the risk is determined by their damage as well as the damage from the adjacent service pipelines.

A Bayesian Network (BN) approach was used to integrate the above damage defects and produce the overall damage probability. BN is favoured in this study because it can be used to model accident scenarios and determine the probabilities of different scenarios using accident prior information. Moreover, the observed damage defects information can be updated to the model.

In this study, a BN model is constructed using historical data. The joint probability of a set of n risk indicators $U = \{R_1, R_1, \dots, R_n\}$ can be given by the product of the conditional probability tables specified in the Bayesian networks as:

$$P(U) = \prod_{i=1}^{n} P(R_i | Pa(R_i))$$

Where $Pa(R_i)$ denotes the parent of R_i in the Bayesian networks;

$P(U)$ denotes the properties of the Bayesian network.

To predict the risk probability of events given the conditions of the occurrence probability of the observed defects (prior), called evidence E, to yield the consequence probability (posterior) using the following equation:

$$P(U|E) = \frac{P(U,E)}{P(E)} = \frac{P(U,E)}{\sum_U P(U,E)}$$

A high-risk heat map is prepared in ArcGIS to display the patterns of the distribution and service pipeline risks. This heat map provides relevant, trustworthy statistics for decision-makers to understand the potential risks related to the pipeline network system. In this study, the kernel density estimation (KDE) is taken for generating the heat map. In statistics, KDE is a non-parametric way to estimate the probability function of a random variable. In this study, we implemented the line KDE (Flahaut et al., 2003) in ArcGIS for estimating the risk probability. The kernel estimator of the density of the risk is defined as:

$$\hat{f}(x) = \frac{1}{nh}\sum_{1}^{n} K(\frac{x - x_i}{h})$$

Where x_i are a set of n random variables with density $f(\mathrm{x})$;

h is the smoothing parameter (bandwidth) that determines the window width of the function;

K denotes the kernel function, which determines the shape of the function, this study employs standard normal density function as the kernel function.

4. Results

Lavallette, Ortley Beach, and Seaside Heights, located in the Barnegat Peninsula in Ocean Country, New Jersey, were selected as the study scope because they took the major hit during hurricane Sandy (Hu and Gong, 2019b). Figure 2 depicts the building damage maps during hurricane sandy. The data is obtained from the FEMA Modelling Task Force (MOTF). Building conditions are classified into four levels: affected, minor, major, and destroyed. Figure 2a displays a kernel density map of the building damage in the entire New Jersey shoreline area. The map is constructed based on the kernel density function, which is introduced in the previous section. Figure 2b depicts a detailed distribution of residential house damage in the abovementioned municipalities.

4.1 Threats measurement results

The proposed method is implemented in ArcGIS and tested in a hurricane Sandy (2012) scenario. Hurricane Sandy (2012) wreaked havoc on the Atlantic shoreline area in 2012, destroying housing and infrastructure. Though no direct incidents are reported to be caused by the pipeline damage, the aging pipeline after the formidable forces from nature (e.g., storm surge, flooding, etc.) are posing life-threatening risks to the people in this area. Identifying the risk of the pipeline system and making corresponding and response planning is a necessity to improve the coastal resilience aftermath of an extreme event.

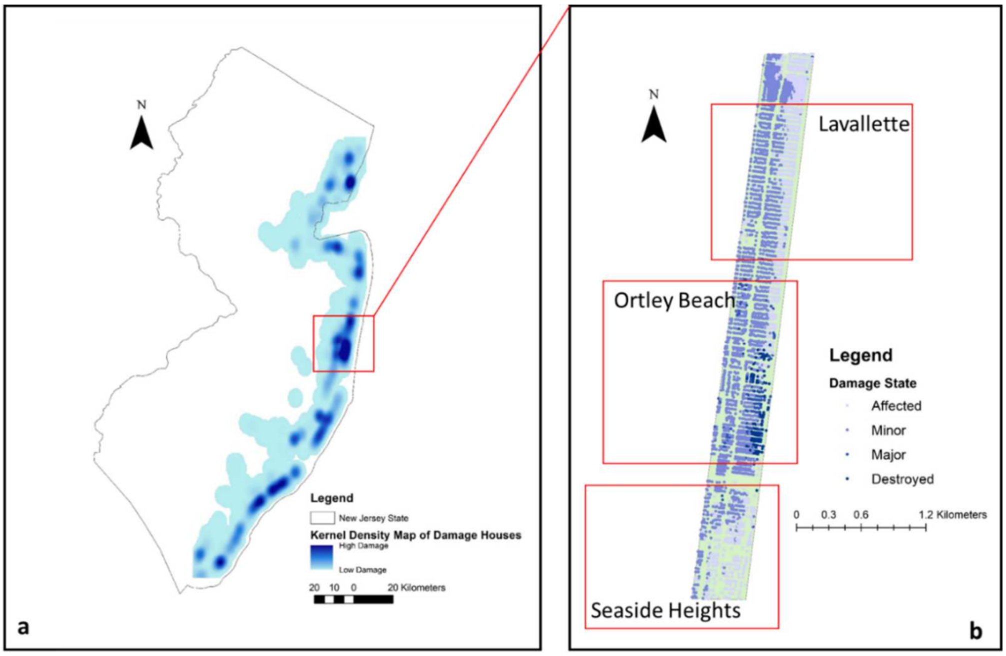

Figure 2 Hurricane Sandy Building Damage Map

4.1.1 Vertical Displacement

The vertical displacement from change detection in the three municipalities before and after hurricane Sandy striked is depicted in Figure 3. The red colors indicate the decrease of elevation height as a result of terrain morphology changes (e.g., dune erosion). The result suggests the dunes in all three communities are subject to substantial erosion as a result of the storm surge. On the other hand, the blue colors indicate the increase in the elevation, which is majorly attributed to the pipeline of foodborne debris, which is consisting of dune sand, vegetation, and other street furniture that is transported by moving water to the inland area. This piling debris could impose additional loading, and resulting in increasing the bending movement of the underground distribution pipeline. In Figure 3, it can be obtained that in Ortley Beach, the flood-borne debris is majorly from the ocean side while in Lavallette, the debris is from the bayside as indicated by the concentration of blue colors (increase in elevation.).

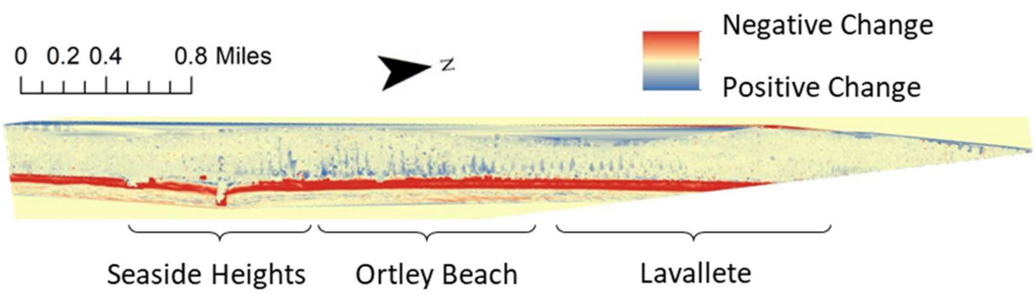

Figure 3 Elevation Change during Hurricane Sandy

4.1.2 Lateral Deformation

Table 2 depicts the rigid body transformation matrix at six random locations including inland, bayside, and oceanfront. In the matrix, $\mathrm{m}_{14}, \mathrm{m}_{24}$ represent a transformation in the x-axis and y-axis respectively. After the transformation of n (n=50) random points are determined, a kernel interpolation analysis is performed in ArcGIS for mapping the Lateral Deformation in the study scope.

Different from the vertical displacement that varies across communities, the lateral deformation significantly reduces from the oceanfront to the bayside. This aligns with the fact that most of the lateral loads are from the ocean side (e.g. wind load, debris flow). The ocean water is continuously eroding the dune, resulting in descending in the crest of the oceanfront dune in Ortley Beach. The breach in the dune forms a channel for high-velocity water to enter. This high-speed water entrains sand and other objects in their path, forming debris flow. Debris flow moves from the oceanfront of Ortely Beach to the Inland area causing significant lateral deformation. Meanwhile, the wind flow pressures can rip off roofing and cause racking of walls, which results in building deformation.

Table 2 Rigid body transformation matrix at different Random Locations

Bayside	$\phi_1 = \begin{pmatrix} 1 & 0 & 0 & -0.017 \\ 0 & 1 & 0 & 0.006 \\ 0 & 0 & 1 & 0.001 \\ 0 & 0 & 0 & 1 \end{pmatrix}, \phi_2 = \begin{pmatrix} 1 & 0 & 0 & 0.065 \\ 0 & 1 & 0 & 0.014 \\ 0 & 0 & 1 & 0.007 \\ 0 & 0 & 0 & 1 \end{pmatrix}$
Inland	$\phi_0 = \begin{pmatrix} 1 & -0.001 & -0.001 & 0.234 \\ 0.001 & 1 & 0 & 0.456 \\ 0.001 & 0 & 1 & -0.120 \\ 0 & 0 & 0 & 1 \end{pmatrix}, \phi_9 = \begin{pmatrix} 1 & 0 & 0 & 0.193 \\ 0 & 1 & 0 & -0.025 \\ 0 & 0 & 1 & -0.005 \\ 0 & 0 & 0 & 1 \end{pmatrix}$
Oceanfront	$\phi_5 = \begin{pmatrix} 1 & 0.002 & 0.009 & 2.1749 \\ -0.002 & 1 & -0.001 & -1.018 \\ -0.009 & 0.001 & 1 & 0.229 \\ 0 & 0 & 0 & 1 \end{pmatrix}, \phi_6 = \begin{pmatrix} 1 & 0.002 & -0.006 & 6.384 \\ -0.002 & 1 & 0 & -0.1625 \\ 0.006 & 0 & 1 & 2.816 \\ 0 & 0 & 0 & 1 \end{pmatrix}$

4.1.3 Flooding

Figure 4 displays the mapping of flooding height. The deep color indicates a higher flooding level while the light color indicates the lower flooding level. Comparatively, the color on the bayside is deeper than the color from the oceanfront, indicating the bayside might be subjected to more server flooding damage. The explanation for this phenomenon is two folds. First, the flood height in the oceanfront is less because the area is under the sheltering protection of the dune structures. By contrast, water is prone to intrude into the inland area from the bayside, where there exists no water breaking or water preventing structures. Second, the ground elevation in the oceanfront is much higher than the bayside. Flooding water is flowing from higher elevations (oceanfront) to lower elevations (bayside) and eventually reaches the lowland.

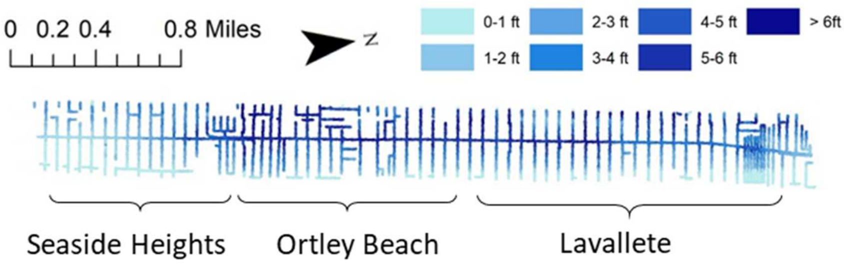

Figure 4 Flooding height map

4.1.4 Aging effect

Figure 5 depicts the KDE-based age distribution map of the pipeline networks. In the figure, the deeper color indicates an elder age while the lighter color indicates a relatively younger age. In all, according to the inventory data, a considerable amount (46.87%) of pipeline ages 40 or older while over 20% of them ages 70 and older in the study area. Particularly, the pipelines were built across multiple decades, leading to varying aging effects on the pipelines. The uneven distribution of the pipelines suggests that we cannot the entire pipeline as a whole for the aging effect analysis, but should be assessed separately according to their construction year to identify high-risk pipelines. This further highlights the need for our aging effect analysis. Specifically, two high-risk areas are identified. First, the northeast end of the Lavallette was identified as the high-aging risk area. This could be the result of a combination of dense and aging pipelines. Second, most of the deep colors are concentrated along the distribution pipeline, suggesting that the distribution pipeline is prone to be subjected to stronger aging risk. All combined, the threats from the aging effect are non-negligible.

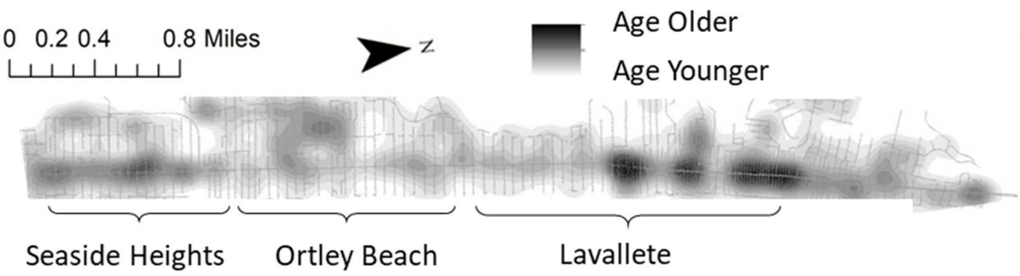

Figure 5 KDE based aging map

4.2 Vulnerability analysis results

In sum, a total of 11 attributes (Table 3), including 7 pipeline characteristics from inventory data and the above four threats, are integrated into a BN model (Farrag and Gong, 2016b) as depicted in Figure 6.

Table 3 Risk analysis attributes

Attributes	Categories
History data	

Pipe Material	(1) Plastic pipe; (2) Steel pipe; (3) Cast iron pipe.
Line Type	(1) Service lines; (2) Main
Pipe Size	(1) <= 1 inch; (2) 1 to 4 inch; (3) 4 to 6 inch; (4) > 6 inch.
Mechanical Coupling	(1)Yes; (2) No; (3) Unknown.
Soil Type	(1) Sand; (2) Silt & Clay; (3) Unknown.
Depth of cover	(1)<= 2 inch; (2) 2 to 4 inch; (3) > 4 inch; (4) Unknown.
Leak History	(1) Low Rate; (2) Medium Rate; (3)High rate.
Disaster Data	
Horizontal Displacement	(1) <12 inch; (3) 12-24 inch; (4) 24-36 inch; (5) 36-48 inch; (6) >48 inch
Vertical Displacement	(1) <12 inch; (3) 12-24 inch; (4) 24-36 inch; (5) 36-48 inch; (6) >48 inch
Length of Displaced soil	(1) Short (<= 30ft); (2) Long (>=30ft); (30 Unknown
Flood Water Level	(1) No Flood; (2)0-6 ft.; (3) >6ft.

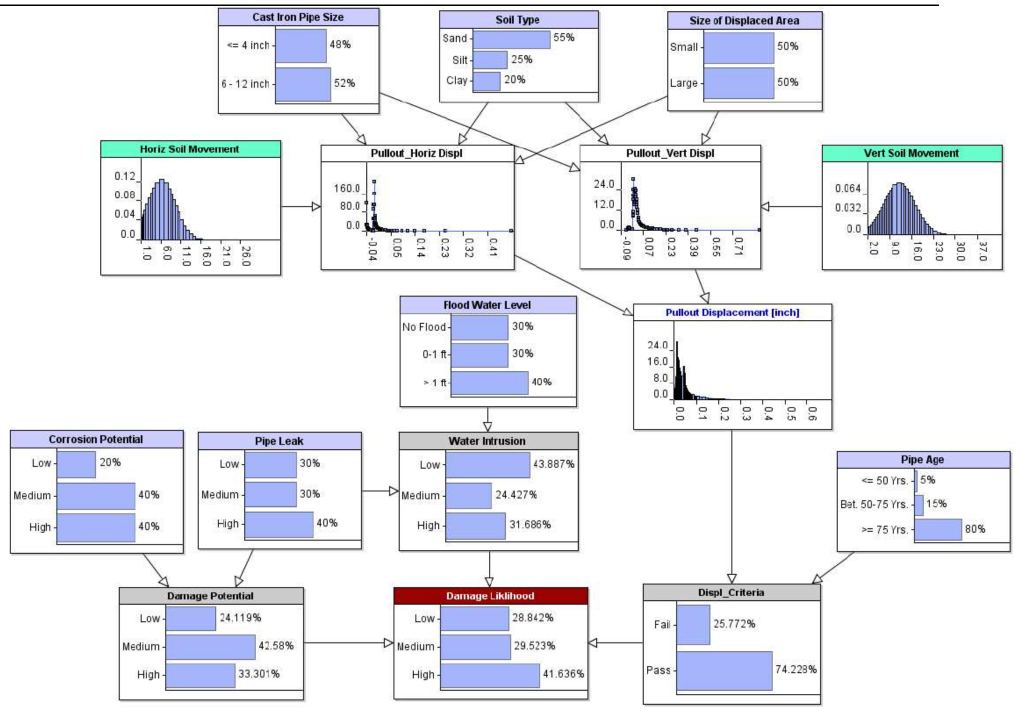

Figure 6 Bayesian network for pipeline risk analysis (adopted from Farrag and Gong (2016a)

To visualize the risk distribution, Figure 7 shows the kernel interpolation map of the high-risk underground pipeline. The deeper color indicates higher risks while the lighter color indicates lower risks. Regarding the distribution, the high-risk pipeline is located in the east end of Lavallette, the entire Ortley Beach as well as the Bayside of the Seaside Heights. These high dense risk pipeline locations can result from different reasons. For instance, the risk of the pipeline in the east end of Lavallette and bayside of the Seaside Heights could have resulted majorly from the aging effect. It is observed in Figure 5, both areas have the densest aging pipeline. On the other hand, in Ortley Beach, the risk could be the result of a combined effort of Vertical Displacement, Lateral Deformation, and flooding. Regarding the type of pipeline, it is observed that the main gas pipelines extending from Ortley beach to Lavallette are attributed to higher risks. In addition to the fact that the main distribution gas pipelines bear greater risk, this implies that the necessity of assessing the risk of the main pipelines from a holistic view: the integrity of the entire main pipelines requires further exploration.

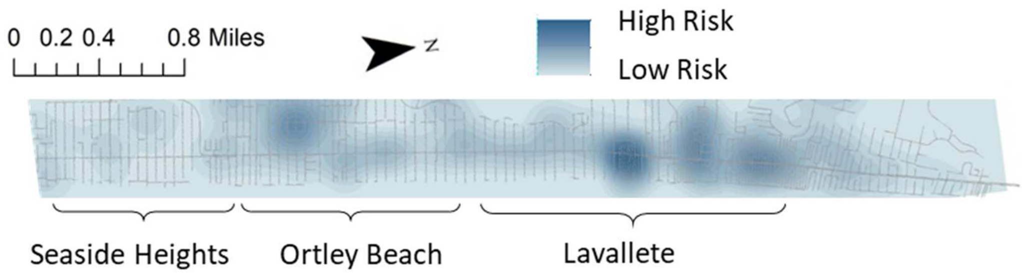

Figure 7 Consequence analysis results

5. Discussion

Traditional pipeline risk analysis has relied on high-precision pipeline detection tools that emphasized accuracy (Fang et al., 2019; Wang et al., 2020), which cannot be extended to enhance the adaptability of the coastal resilience because the requirements are deemed different. Improving adaptability requires identifying the vulnerability of the community within a narrow time window. In light of this, the accuracy is less a concern because the high accuracy of the high-precision pipeline detection tools is often accompanied by extensive labor and intensitive time (Zakikhani et al., 2020), which impose additional difficulties on the vulnerability analysis. Therefore, we argued that the adaptability-centric pipeline risk analysis has different requirements. First, Rodríguez-Espíndola et al. (2018) argued that improvisation is important in disaster response, which is based on speedy assessment. Put differently, the rapidity of the assessment could be a premise for any further decision-making. Furthermore, Quarantelli and Dynes (1977) stressed that the appropriateness of response is as important as the speed of response. Here, appropriateness refers to the applicability (Elaine Daily and Padjen, 2010), and operability (Huang and Lien, 2012) of the assessment. In terms of applicability, Xie and Tian (2018) argued the anticipation of high-precision defect detection tools (e.g., ultrasonic, magnetic flux) is simply impossible during disaster response because these tools are considered expensive, time-consuming, and unsafe to operate. In terms of operability, adaptability-centric pipeline vulnerability tools require stable and productive tools. To this end, rapidity, applicability, and operability are deemed appropriate for addressing the pipeline risk need in disaster response.

The proposed methodology in this study is carried out to address the above three requirements. Regarding the rapidity, compared to the labor-intensive and time-consuming pipeline detection tools (Alobaidi et al., 2015; Gloria et al., 2009), the proposed method is built high efficiency remote sensing LiDAR data (Hu and Gong, 2018), which has substantial progress in the time efficiency in capture the real-time or near real-time damage defects. Regarding the applicability, the four threats that we considered for the vulnerability analysis are considered as the major threats to the pipeline system after hurricanes which are evidenced in other work such as (Dahire et al., 2018; Li et al., 2017; Wang et al., 2020; Zeng et al., 2019). Regarding the operability, the proposed method is built by integrating a serial of already-in-place geospatial analysis tools (e.g., Iterative Closest Point, Kernel Interpolation), which has already proved stable and productive in numerous fields (Flahaut et al., 2003; Nissen et al., 2012).

The contribution of this study is two-fold. Theoretically, this study complements existing literature on coastal resilience by emphasizing the need for underground gas pipeline risk assessment after a hurricane strikes, which enhances our understanding of improving the adaptability perspective of coastal resilience. Specifically for coastal resilience applications, we further summarized three requirements (rapidity, applicability, and operability), which may point to another branch of pipeline risk analysis. Practically, compared to traditional pipeline risk analysis that focuses on accuracy, we leveraged LiDAR data and in place geospatial tools in ArcGIS for the timely risk assessment. We further developed methods to identify the risk of pipeline based on four facets of damage mechanisms (vertical displacement, lateral deformation, flooding, and aging effect). This study provides a preliminary attempt to exploit remote sensing data for assessing pipeline risks after a disaster, which is expected to encourage the emergence of more relevant research.

There are also limitations of this study. Due to the lacking of precise risk data, we were unable to pairwise verify our analytic result with the actual risk. However, we argue that the four geometry changes based on damage sources deem reasonable representing the damage mechanism after hurricanes. First, all the houses are subjected to severe wind load from the ocean side. By comparison, houses (Lavallette and Seaside Heights) under the protection of a strong dune are evidenced with less server damage than those (Oretely Beach) without the protection. Second, flooding load attributes another damage source. In Lavallette and Seaside Heights, the majority of damage is concentrated on the bayside rather than the oceanfront, indicating that flooding force could be the main cause. Moreover, the damage in the house, the erosion of the sand, the formulation of debris flow would inevitably cause vertical soil movement, imposing threats to the gas pipeline system beneath the ground. Last, from the inventory data, more than 50% of the pipelines aged 40 years and older as depicted in Figure 5, the risk of the aging pipeline is self-explanatory.

Regarding the future work, in the absence of matching datasets, we are not able to quantitatively identify the accuracy of the analysis in this analysis, which is worthy of further investigation. Meanwhile, given that the airborne datasets that we used are considered as relatively low density (Hodgson and Bresnahan, 2004), the ability of accuracy improvement if higher quantity datasets are deployed determines the extendibility of the proposed method to broader application scenarios. Furthermore, due to the limitation of LiDAR accuracy, small deformation damage defects (e.g., crack) (Laefer et al., 2010) cannot be readily identified. However, these minor defects could also create huge risks to the pipeline system, which is to be addressed in future work.

6. Conclusions

This study is motivated by practical needs. Based on the literature analysis, we identified a gap that the extant coastal resilience research that pipeline risk analysis is largely understudied. Specifically, while the capability of community resilience can be enhanced using high-precision defect detection tools, the studies on the adaptability perspective of community resilience are understudied. To improve the adaptability, we first summarized three requirements for identifying the pipeline vulnerability in disaster response including, rapidity, applicability, and operability. Drawing upon these requirements, we further investigated the hurricane-induced pipeline damage and identified four facets of the damage mechanism including (1) vertical displacement, (2) lateral deformation, (3) flooding, and (4) aging effect. To identify the vulnerability of the pipeline, the risk associated with these four damage mechanisms were assessed by integrating remote sensing LiDAR data and geospatial analytic tools in ArcGIS. The methodology is validated through a hurricane Sandy case study in Ocean County, New Jersey. We found that the proposed method not only satisfies the above three requirements in disaster response, but also aligns with the observed hurricane-induced geometry change patterns, and therefore deem appropriate for the rapid assessment of pipeline risk after extreme weather events.

Data Availability Statement

Airborne LiDAR data used in this study are available online from NOAA digital Coast (https://coast.noaa.gov/digitalcoast/) in accordance with funder data retention policies. Some or all data, models, or codes that support the findings of this study are available from the corresponding author upon reasonable request. The GIS toolbox code that supports the findings of this study is available from the corresponding author upon reasonable request.

Reference

Aljaroudi, A., Khan, F., Akinturk, A., Haddara, M., Thodi, P., 2015. Risk assessment of offshore crude oil pipeline failure. Journal of Loss Prevention in the Process Industries 37, 101-109.

Alobaidi, W.M., Alkuam, E.A., Al-Rizzo, H.M., Sandgren, E., 2015. Applications of ultrasonic techniques in oil and gas pipeline industries: A review. American Journal of Operations Research 5, 274.

Barbier, E.B., 2014. A global strategy for protecting vulnerable coastal populations. Science 345, 1250-1251.

Cagno, E., Caron, F., Mancini, M., Ruggeri, F., 2000. Using AHP in determining the prior distributions on gas pipeline failures in a robust Bayesian approach. Reliability Engineering & System Safety 67, 275-284.

Campbell, M.J., Dennison, P.E., Hudak, A.T., Parham, L.M., Butler, B.W., 2018. Quantifying understory vegetation density using small-footprint airborne lidar. Remote sensing of environment 215, 330-342.

Canaz, S., Karsli, F., Guneroglu, A., Dihkan, M., 2015. Automatic boundary extraction of inland water bodies using LiDAR data. Ocean & Coastal Management 118, 158-166.

Carvalho, A., Rebello, J., Sagrilo, L., Camerini, C., Miranda, I., 2006. MFL signals and artificial neural networks applied to detection and classification of pipe weld defects. Ndt & E International 39, 661-667.

Cevik, E., Topal, T., 2003. GIS-based landslide susceptibility mapping for a problematic segment of the natural gas pipeline, Hendek (Turkey). Environmental geology 44, 949-962.

Chen, A.Y., Peña-Mora, F., Ouyang, Y., 2011. A collaborative GIS framework to support equipment distribution for civil engineering disaster response operations. Automation in Construction 20, 637-648.

Chen, H., Zuo, M.J., Wang, X., Hoseini, M.R., 2010. An adaptive Morlet wavelet filter for time-of-flight estimation in ultrasonic damage assessment. Measurement 43, 570-585.

Dahire, S., Tahir, F., Jiao, Y., Liu, Y., 2018. Bayesian Network inference for probabilistic strength estimation of aging pipeline systems. International Journal of Pressure Vessels and Piping 162, 30-39.

Davis, P., Dubois, J., Olcese, A., Uhlig, F., Larivé, J., Martin, D., 2006. Performance of European cross-country oil pipelines. Statistical summary of reported spillages 54.

Dixon, S., Burrows, S.E., Dutton, B., Fan, Y., 2011. Detection of cracks in metal sheets using pulsed laser generated ultrasound and EMAT detection. Ultrasonics 51, 7-16.

Elaine Daily, R., Padjen, P., 2010. A review of competencies developed for disaster healthcare providers: limitations of current processes and applicability. Prehospital and disaster medicine 25, 387-395.

Fang, W., Wu, J., Bai, Y., Zhang, L., Reniers, G., 2019. Quantitative risk assessment of a natural gas pipeline in an underground utility tunnel. Process safety progress 38, e12051.

Farrag, K., Gong, J., 2016a. Risk Analysis of Natural Gas Distribution Lines Subjected to Natural Forces, Transportation Research Board 95th Annual MeetingTransportation Research Board.

Farrag, K., Gong, J., 2016b. Risk Analysis of Natural Gas Distribution Lines Subjected to Natural Forces, Transportation Research Board 95th Annual Meeting.

Fiedrich, F., Gehbauer, F., Rickers, U., 2000. Optimized resource allocation for emergency response after earthquake disasters. Safety science 35, 41–57.

Flahaut, B., Mouchart, M., San Martin, E., Thomas, I., 2003. The local spatial autocorrelation and the kernel method for identifying black zones: A comparative approach. Accident Analysis & Prevention 35, 991-1004.

Font, M., Amorese, D., Lagarde, J.-L., 2010. DEM and GIS analysis of the stream gradient index to evaluate effects of tectonics: the Normandy intraplate area (NW France). Geomorphology 119, 172-180.

Glisic, B., Yao, Y., 2012. Fiber optic method for health assessment of pipelines subjected to earthquake-induced ground movement. Structural Health Monitoring 11, 696-711.

Gloria, N., Areiza, M., Miranda, I., Rebello, J., 2009. Development of a magnetic sensor for detection and sizing of internal pipeline corrosion defects. NDT & e International 42, 669-677.
Gunes, A.E., Kovel, J.P., 2000. Using GIS in emergency management operations. Journal of Urban Planning and Development 126, 136-149.
Han, Z.Y., Weng, W.G., 2011. Comparison study on qualitative and quantitative risk assessment methods for urban natural gas pipeline network. Journal of hazardous materials 189, 509-518.
Hassanzadeh, P., Lee, C.-Y., Nabizadeh, E., Camargo, S.J., Ma, D., Yeung, L.Y., 2020. Effects of climate change on the movement of future landfalling Texas tropical cyclones. Nature communications 11, 1-9.
Hatzikyriakou, A., Lin, N., Gong, J., Xian, S., Hu, X., Kennedy, A., 2015. Component-based vulnerability analysis for residential structures subjected to storm surge impact from Hurricane Sandy. Natural Hazards Review 17, 05015005.
Hirao, M., Ogi, H., 1999. An SH-wave EMAT technique for gas pipeline inspection. Ndt & E International 32, 127-132.
Hodgson, M.E., Bresnahan, P., 2004. Accuracy of airborne LiDAR-derived elevation. Photogrammetric Engineering & Remote Sensing 70, 331-339.
Hu, X., Gong, J., 2018. Advancing Smart and Resilient Cities with Big Spatial Disaster Data: Challenges, Progress, and Opportunities, Data Analytics for Smart Cities. Auerbach Publications, pp. 53-90.
Hu, X., Gong, J., 2019a. Framework for prioritizing geospatial data processing tasks during extreme weather events. Advanced Engineering Informatics 39, 157-169.
Hu, X., Gong, J.J.A.E.I., 2019b. Framework for prioritizing geospatial data processing tasks during extreme weather events. 39, 157-169.
Huang, J.-S., Lien, Y.-N., 2012. Challenges of emergency communication network for disaster response, 2012 IEEE International Conference on Communication Systems (ICCS). IEEE, pp. 528-532.
Huang, X., Song, Y., Hu, X., 2021. Deploying Spatial Data for Coastal Community Resilience: A Review from the Managerial Perspective. International Journal of Environmental Research and Public Health 18, 830.
Jamshidi, A., Yazdani-Chamzini, A., Yakhchali, S.H., Khaleghi, S., 2013. Developing a new fuzzy inference system for pipeline risk assessment. Journal of loss prevention in the process industries 26, 197-208.
Jin, Q., Sun, Z.Y., Guo, W.N., 2014. Experimental and finite element study on the fatigue growth of a semi-elliptical surface crack in a X80 pipeline steel specimen, Applied Mechanics and Materials. Trans Tech Publ, pp. 3026-3029.
Jo, Y.-D., Ahn, B.J., 2005. A method of quantitative risk assessment for transmission pipeline carrying natural gas. Journal of hazardous materials 123, 1-12.
Kucera, P.A., Krajewski, W.F., Young, C.B., 2004. Radar beam occultation studies using GIS and DEM technology: An example study of Guam. Journal of Atmospheric and Oceanic Technology 21, 995-1006.
Kumar, G.A., Patil, A.K., Patil, R., Park, S.S., Chai, Y.H., 2017. A LiDAR and IMU integrated indoor navigation system for UAVs and its application in real-time pipeline classification. Sensors 17, 1268.
Laefer, D.F., Gannon, J., Deely, E., 2010. Reliability of crack detection methods for baseline condition assessments. Journal of Infrastructure Systems 16, 129-137.

Lee, J.-R., Jeong, H., Ciang, C.C., Yoon, D.-J., Lee, S.-S., 2010. Application of ultrasonic wave propagation imaging method to automatic damage visualization of nuclear power plant pipeline. Nuclear engineering and design 240, 3513-3520.

Lee, L.H., Rajkumar, R., Lo, L.H., Wan, C.H., Isa, D., 2013. Oil and gas pipeline failure prediction system using long range ultrasonic transducers and Euclidean-Support Vector Machines classification approach. Expert Systems with Applications 40, 1925-1934.

Li, S., Duan, Q., Zhang, H., Wang, J., 2017. Failure analysis of the floating pipeline with defect under flooding load. Engineering failure analysis 77, 65-75.

Lin, N., Emanuel, K., Oppenheimer, M., Vanmarcke, E., 2012. Physically based assessment of hurricane surge threat under climate change. Nature Climate Change 2, 462–467.

Linnenluecke, M.K., McKnight, B., 2017. Community resilience to natural disasters: the role of disaster entrepreneurship. Journal of Enterprising Communities: People and Places in the Global Economy.

Liu, Y., Gebremeskel, S., De Smedt, F., Hoffmann, L., Pfister, L., 2003. A diffusive transport approach for flow routing in GIS-based flood modeling. Journal of Hydrology 283, 91-106.

Nissen, E., Krishnan, A.K., Arrowsmith, J.R., Saripalli, S., 2012. Three-dimensional surface displacements and rotations from differencing pre-and post-earthquake LiDAR point clouds. Geophysical Research Letters 39.

NTSB, 1996. Safety Recommendation P-96-022. National Transportation Safety Board.

Piciarelli, C., Avola, D., Pannone, D., Foresti, G.L., 2018. A vision-based system for internal pipeline inspection. IEEE Transactions on Industrial Informatics 15, 3289-3299.

Quarantelli, E.L., Dynes, R.R., 1977. Response to social crisis and disaster. Annual review of sociology 3, 23-49.

Rango, A., Chopping, M., Ritchie, J., Havstad, K., Kustas, W., Schmugge, T., 2000. Morphological characteristics of shrub coppice dunes in desert grasslands of southern New Mexico derived from scanning LIDAR. Remote Sensing of Environment 74, 26-44.

Rodríguez-Espíndola, O., Albores, P., Brewster, C., 2018. Decision-making and operations in disasters: challenges and opportunities. International Journal of Operations & Production Management.

Roper, W.E., Dutta, S., 2005. Remote sensing and GIS applications for pipeline security assessment, 2005 ESRI User Conference Proceedings.

Roper, W.E., Dutta, S., 2006. Oil spill and pipeline condition assessment using remote sensing and data visualization management systems, Freshwater Spills Symposium, Natural Disasters, Human Error, and Equipment Failure-Causes for Major Inland Oil Spills and the Resulting Multifaceted Response.

Saha, S., Mukhopadhyay, S., Mahapatra, U., Bhattacharya, S., Srivastava, G., 2010. Empirical structure for characterizing metal loss defects from radial magnetic flux leakage signal. Ndt & E International 43, 507-512.

Saniie, J., Oruklu, E., Yoon, S., 2012. System-on-chip design for ultrasonic target detection using split-spectrum processing and neural networks. IEEE transactions on ultrasonics, ferroelectrics, and frequency control 59, 1354-1368.

Shi, Y., Zhang, C., Li, R., Cai, M., Jia, G., 2015. Theory and application of magnetic flux leakage pipeline detection. Sensors 15, 31036-31055.

Sinha, S.K., McKim, R.A., 2007. Probabilistic based integrated pipeline management system. Tunnelling and underground space technology 22, 543-552.

Standard, A., 2001. 1160 Managing System Integrity for Hazardous Liquid Pipelines. Firs Edition, November.
Tao, C.V., Hu, Y., 2002. Assessment of airborne lidar and imaging technology for pipeline mapping and safety applications, Integrated remote sensing at the global, regional and local scale, ISPRS commission I mid-term symposium in conjunction with Pecora 15/land satellite information IV conference proceedings.
Tatui, F., Pirvan, M., Popa, M., Aydogan, B., Ayat, B., Gormus, T., Korzinin, D., Vaidianu, N., Vespremeanu-Stroe, A., Zainescu, F., Kuznetsov, S., Preoteasa, L., Shtremel, M., Saprykina, Y., 2019. The Black Sea coastline erosion: Index-based sensitivity assessment and management-related issues. Ocean & Coastal Management 182, 17.
Tee, K.F., Khan, L.R., Chen, H.P., Alani, A.M., 2014. Reliability based life cycle cost optimization for underground pipeline networks. Tunnelling and Underground Space Technology 43, 32-40.
Ting, M., Kossin, J.P., Camargo, S.J., Li, C., 2019. Past and future hurricane intensity change along the US east coast. Scientific reports 9, 1-8.
Toprak, S., Nacaroglu, E., Koc, A., O'Rourke, T., Hamada, M., Cubrinovski, M., Van Ballegooy, S., 2018. Comparison of horizontal ground displacements in Avonside area, Christchurch from air photo, LiDAR and satellite measurements regarding pipeline damage assessment. Bulletin of Earthquake Engineering 16, 4497-4514.
Toprak, S., Taskin, F., 2007. Estimation of earthquake damage to buried pipelines caused by ground shaking. Natural hazards 40, 1-24.
Tran, P., Shaw, R., Chantry, G., Norton, J., 2009. GIS and local knowledge in disaster management: a case study of flood risk mapping in Viet Nam. Disasters 33, 152-169.
Vanaei, H., Eslami, A., Egbewande, A., 2017. A review on pipeline corrosion, in-line inspection (ILI), and corrosion growth rate models. International Journal of Pressure Vessels and Piping 149, 43-54.
Wang, K., Liu, Z., Qian, X., He, Y., 2020. Dynamic characteristics and damage recognition of blast-induced ground vibration for natural gas transmission pipeline and its integrated systems. Mechanical Systems and Signal Processing 136, 106472.
Wang, S., Toumi, R., 2021. Recent migration of tropical cyclones toward coasts. Science 371, 514-517.
Xie, M., Tian, Z., 2018. A review on pipeline integrity management utilizing in-line inspection data. Engineering Failure Analysis 92, 222-239.
Yuhua, D., Datao, Y., 2005. Estimation of failure probability of oil and gas transmission pipelines by fuzzy fault tree analysis. Journal of loss prevention in the process industries 18, 83-88.
Zakikhani, K., Nasiri, F., Zayed, T., 2020. A review of failure prediction models for oil and gas pipelines. Journal of Pipeline Systems Engineering and Practice 11, 03119001.
Zeng, X., Dong, F.-f., Xie, X.-d., Du, G.-f., 2019. A new analytical method of strain and deformation of pipeline under fault movement. International Journal of Pressure Vessels and Piping 172, 199-211.
Zerger, A., Smith, D.I., 2003. Impediments to using GIS for real-time disaster decision support. Computers, environment and urban systems 27, 123-141.
Zhang, K., Chen, S.-C., Whitman, D., Shyu, M.-L., Yan, J., Zhang, C., 2003. A progressive morphological filter for removing nonground measurements from airborne LIDAR data. IEEE transactions on geoscience and remote sensing 41, 872-882.

Zhou, Z., Gong, J., Hu, X., 2019. Community-scale multi-level post-hurricane damage assessment of residential buildings using multi-temporal airborne LiDAR data. Automation in Construction 98, 30-45.
Zhou, Z., Gong, J., Roda, A., Farrag, K., 2016a. Multiresolution change analysis framework for postdisaster assessment of natural gas pipeline risk. Transportation research record 2595, 29-39.
Zhou, Z., Gong, J., Roda, A., Farrag, K., 2016b. Multiresolution Change Analysis Framework for Postdisaster Assessment of Natural Gas Pipeline Risk. Transportation Research Record: Journal of the Transportation Research Board, 29-39.
Zou, L., Ren, A.-Z., Zhang, X., 2006. GIS-based evacuation simulation and rescue dispatch in disaster. Ziran Zaihai Xuebao/ Journal of Natural Disasters 15, 141-145.

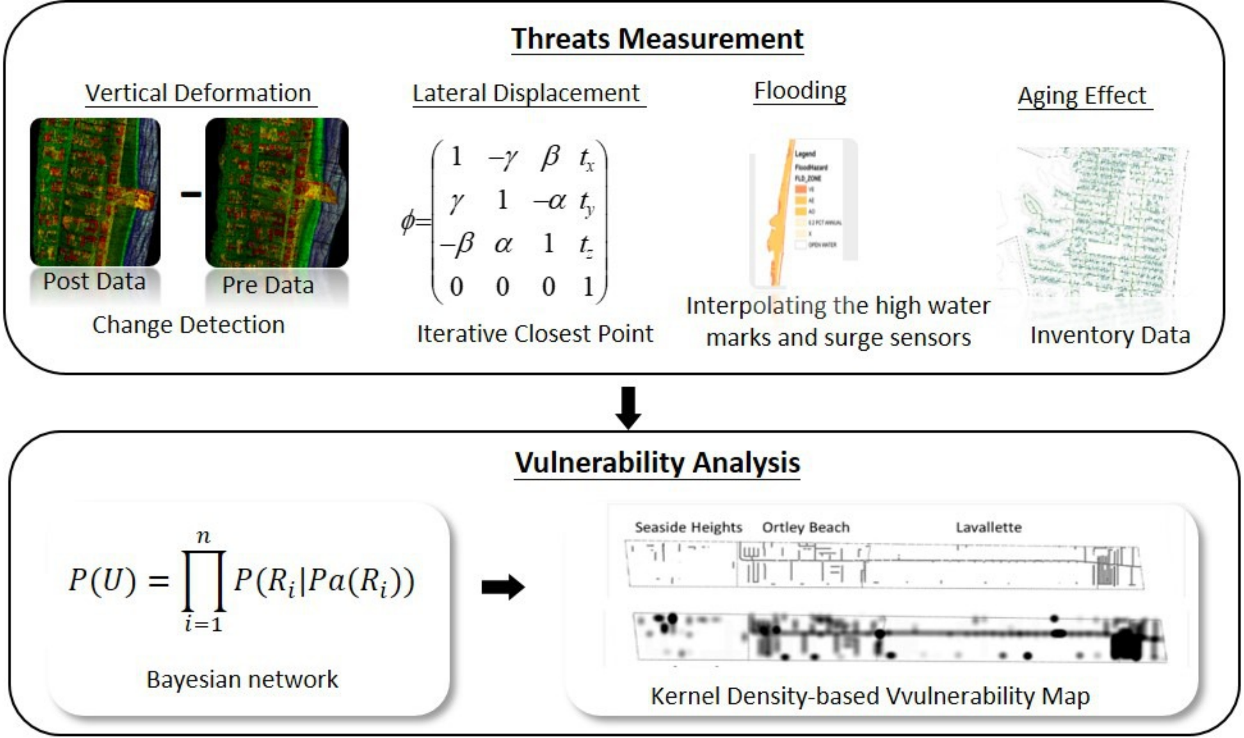

Vulnerability analysis of underground gas pipeline system after hurricanes using LiDAR data